

Shigeru Yamauchi · Yasuji Kurimoto

## Raman spectroscopic study on pyrolyzed wood and bark of Japanese cedar: temperature dependence of Raman parameters

Received: January 28, 2002 / Accepted: June 14, 2002

**Abstract** Raman spectra were measured for Japanese cedar wood and bark pyrolyzed in a nitrogen atmosphere at various temperatures (200°–1100°C). Two characteristic bands, near 1340 and 1590 cm<sup>-1</sup>, denoted as the D-band and G-band due to graphitic carbon, respectively, appeared on all the spectra; and the spectral features changed markedly with increasing heat-treatment temperature (HTT). The Raman parameters (band position, band width, D/G ratio) of the bands were deconvolved using of a curve-fitting method. There was no significant difference in the values of the parameters between the wood and bark. The D-band position and the G-band width showed a marked HTT dependence in the region of 400°–800°C. We described the correlations of the Raman parameters with HTT and investigated the availability of Raman spectroscopy as a means for evaluating HTT.

**Key words** Raman spectroscopy · Japanese cedar · Bark · Pyrolysis · Heat-treatment temperature

### Introduction

During the last decade there was an appreciable worldwide effort to use natural resources more effectively and to recycle them. Therefore, the utilization of bark, low quality wood, and waste timber has become an important subject for discussion. Charcoal prepared from lignocellulosics in particular has attracted much attention and has been investigated not as a fuel but as an adsorbent. We previously explored the suitability of charcoal produced from the bark of Japanese cedar (*Cryptomeria japonica* D. Don) as an adsorbent and reported that it is a good scavenger for halogenated organic compounds in water.<sup>1,2</sup>

A number of Raman studies on carbonaceous materials have been reported since Tuinstra and Koenig<sup>3</sup> studied the Raman spectra of several kinds of graphite. Raman spectroscopy has become an important technique for characterizing materials such as diamond-like carbon because most of the Raman spectra of these materials exhibit two prominent and several other bands in the spectral region 1000–1800 cm<sup>-1</sup>. Although the assignments of Raman bands appearing in this region are still controversial, two characteristic bands, usually classified as the D-band and the G-band by wavenumber, have been regarded as a source of information on the molecular structure and chemical bonding of carbon atoms in carbonaceous materials. The D- and G-bands usually appear near 1340 and 1580 cm<sup>-1</sup>, respectively. Both bands are generally attributed to graphitic sp<sup>2</sup>-bonded carbon; and the D-band is thought to arise from a fairly disordered or distorted structure at the edge of the microcrystallite. In most of the Raman spectroscopic studies, the properties of carbonaceous materials have been discussed according to this attribution.

Despite the wide use of the Raman technique for carbonaceous materials, there have been only a few Raman studies on the thermal degradation or carbonization of wood.<sup>4,5</sup> This is probably because, with conventional Raman analysis, fluorescence arising from visible laser irradiation of raw or low-temperature-treated lignocellulosics frequently prevents one from obtaining a satisfactory spectrum. However, for the heat-treated samples in this study, the hindrance of the fluorescence induced from He-Ne laser irradiation was not fatal, and the Raman spectra were sufficiently good to be analyzed.

In the previous study,<sup>4</sup> we reported marked changes in the Raman spectroscopic features of Japanese cedar bark with increasing heat-treatment temperature (HTT) and suggested that further Raman spectroscopic investigation would make it possible to estimate the HTT. This technique for estimating HTT is expected to be useful for the quality control of charcoal. The main purpose here is to evaluate the availability of Raman spectroscopy as a tool for estimating HTT. In this article, we present Raman spectroscopic parameters (band width, band position, D/G ratio) ob-

S. Yamauchi (✉) · Y. Kurimoto  
Institute of Wood Technology, Akita Prefectural University, 11-1  
Kaieisaka, Noshiro 016-0876, Japan  
Tel. +81-185-52-6984; Fax +81-185-52-6976  
e-mail: sigeru@iwt.akita-pu.ac.jp

tained with a curve-fitting method for both D- and G-bands in heat-treated Japanese cedar and show the HTT dependence of the parameters.

## Experimental

### Materials

The wood (xylem) and bark used in this study were taken from an 80-year old Japanese cedar grown in Akita Prefecture, Japan. Air-dried wood and bark were ground into powder using a Wiley mill, and the powder (12 g) was placed in a porcelain crucible. The crucible was put in an iron vessel and heated in an electric oven under a nitrogen atmosphere. For all heating runs, it took 30–40 min to reach the desired temperature, which varied from 200°C to 1100°C at intervals of 100°C. The samples were maintained in the crucible at the desired temperature for 3 h and then cooled to room temperature.

### FT-Raman spectra of untreated samples

Fourier transform (FT)-Raman spectra of the raw (untreated) Japanese cedar wood and bark were obtained with a JEOL JIR 7000W spectrometer connected to an RS-RSU-200 Raman module in a back-scattering geometry. Excitation was at 1064.1 nm irradiation from an Nd<sup>3+</sup>:YAG laser, and the beam power was about 220 mW. To obtain good-quality spectra, more than 1000 scans were required at about 2 cm<sup>-1</sup> intervals (ca. 4 cm<sup>-1</sup> spectral resolution).

### Raman spectra of heat-treated samples

Raman spectra of the heat-treated Japanese cedar wood and bark were recorded at room temperature using a Renishaw Raman Imaging Microscope System 1000 equipped with an air-cooled CCD detector. A He-Ne laser (632.8 nm) was adopted as the excitation source. Back-scattered Raman signals were collected through a microscope and holographic notch filters in the range of 400–3600 cm<sup>-1</sup> with a spectral resolution of 2 cm<sup>-1</sup>. The laser power was kept at about 20 mW to prevent irreversible thermal damage to the samples. The Raman measurements were carried out at more than five points on each sample. The wavenumber was calibrated using the 460 cm<sup>-1</sup> line of carbon tetrachloride, the 520 cm<sup>-1</sup> line of a silicon wafer, and the 1332 cm<sup>-1</sup> line of diamond.

### Curve fitting of Raman spectra

The Raman data were analyzed using the software package GRAMS/386 (Galactic Industries, Salem, NH, USA). After baseline corrections, Raman parameters (band positions, widths, heights, areas) were determined by curve fitting based on the Levenberg-Marquardt method. A component of a set of overlapping bands was regarded as a linear com-

position of Gaussian and Lorentzian ( $f(x) = a G(x) + (1 - a)L(x)$ ,  $0 \leq a \leq 1$ ), because a poor fit was obtained with only one of the two functions. The curve fitting of the Raman spectra of the samples heat-treated at 200°C or more was performed with two- and four-component bands, respectively.

## Results and discussion

### FT-Raman spectra of raw wood and bark

Although a number of Raman spectroscopic studies of wood (xylem) have been reported recently, none has examined the Raman spectrum for the raw bark of any wood species. In the present study, an attempt was made to measure the Raman spectra of Japanese cedar bark. Good spectra for inner bark were obtained without difficulty; but for the outer bark, background fluorescence prevented us from observing the Raman effect.

Figure 1 shows the FT-Raman spectra of Japanese cedar earlywood in sapwood and inner bark in the 500–2000 cm<sup>-1</sup> region. The Raman band positions of the earlywood (Fig. 1a) were independent of the location of measured points in the wood samples, as reported previously.<sup>6–8</sup> There were, however, considerable differences in the intensity of the Raman bands between earlywood and latewood. In

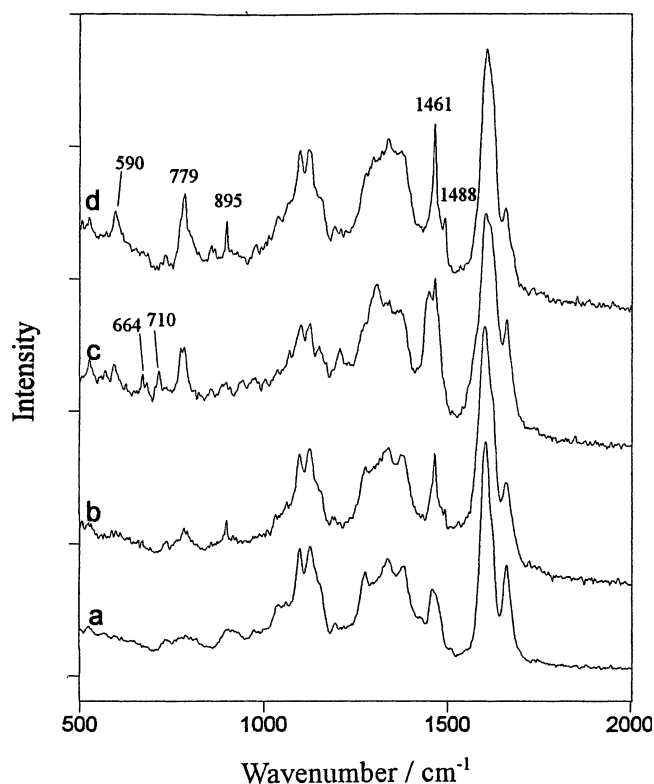


**Fig. 1.** Fourier transform (FT)-Raman spectra of the raw wood and the raw inner bark of Japanese cedar: a, earlywood; b, inner bark 1; c, inner bark 2; d, inner bark 3

contrast, the Raman line shapes of inner bark varied apparently with the measured point in a sample. Three representative spectra of inner bark are given in Fig. 1b–d.

Several Raman bands (e.g., 590, 779, and 895  $\text{cm}^{-1}$ ) that were not observed for the sapwood appeared in the inner bark spectra, and most of them varied markedly in intensity but scarcely shifted in wavenumber among the three spectra. It is generally accepted that bark contains more suberin and wax, which have relatively long normal aliphatic chains of type  $\text{—(CH}_2\text{)}_n\text{—}$  than xylem.<sup>9–11</sup> It is therefore likely that the strong bands at 1461  $\text{cm}^{-1}$  were due to a scissor vibration of the  $\text{—CH}_2\text{—}$  group. Some bands from 650 to 1100  $\text{cm}^{-1}$  could be attributable to C—C stretching vibrations, and others appearing in the same region can probably be assigned to skeletal vibrations of substituted benzene rings because bark contains more lignin-like compounds that have phenolic groups than xylem. In addition, for the wood and bark samples heat-treated above 200°C, irradiation of 1064.1 nm light induced intense fluorescence.

#### Raman spectra of the heat-treated wood and bark

A large portion of the bark heat-treated at 200°C remained nearly raw because its weight loss was only 4.4%.<sup>1</sup> Therefore, the Raman measurements for this sample were carried out only on the parts that had turned black (seen by microscopy). The bark samples heat-treated above 300°C were completely black to the naked eye. In contrast to the bark, the wood samples heat-treated at 200°C scarcely changed color, and strong fluorescence hindered us from obtaining a Raman spectrum. Above 300°C, the wood samples also turned black and showed the same spectral features as the bark samples at each HTT.

Figure 2 shows typical Raman spectra in the 600–2000  $\text{cm}^{-1}$  region of the bark heat-treated at 200–1100°C, whose baselines were corrected so they were free from distortion caused by fluorescence. The influence of fluorescence diminished with increasing HTT and was negligible above 800°C. All the spectra exhibited two broad bands near 1340  $\text{cm}^{-1}$  (D-band) and 1590  $\text{cm}^{-1}$  (G-band). In addition, above 700°C a shoulder was discernible at about 1160  $\text{cm}^{-1}$ .

It has been reported that the thermal degradation or depolymerization of hemicellulose, cellulose, and lignin in wood begins at 200–250°C, 240–350°C, and 280–500°C, respectively.<sup>12</sup> It is well established that bark usually contains more low molecular weight oligosaccharides and phenolic compounds than wood. The bark of Japanese cedar is no exception,<sup>13,14</sup> and some of the compounds in the bark are probably pyrolyzed to elemental or nearly elemental carbon at temperatures below 200°C.

According to infrared spectroscopic studies on the pyrolysis of wood,<sup>15,16</sup> a large proportion of the CH and OH groups should remain in the bark heat-treated up to 500°C. However, no Raman bands due to atomic groups containing H or O were observed for any heat-treated bark samples in the region of 400–3600  $\text{cm}^{-1}$ . Therefore, any discussion of the Raman spectra obtained from 632.8 nm excitation

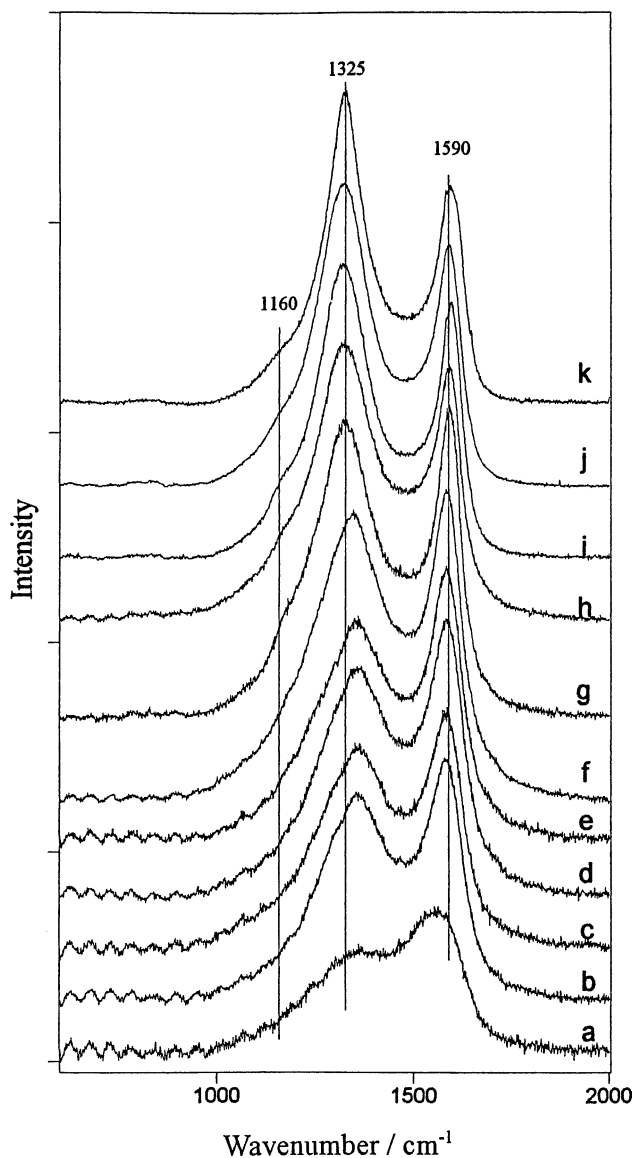


**Fig. 2.** Raman spectra of Japanese cedar bark heat-treated at various temperatures: a, 200°C; b, 300°C; c, 350°C; d, 400°C; e, 500°C; f, 600°C; g, 700°C; h, 800°C; i, 900°C; j, 1000°C; k, 1100°C

should be based on the assumption that they provide information only about the assembly of elemental carbon.

As seen in Fig. 2, the line shapes of both the D- and G-bands varied significantly with HTT. In most Raman spectroscopic studies on carbonaceous materials, the D-band is attributed to  $\text{sp}^2$ -bonded carbon. The G- and D-bands observed in polycrystalline graphite are due to a Brillouin zone-center phonon (lattice vibration) and a zone-edge phonon that is able to form in the reduced-symmetry environment at the edges of the microcrystallite, respectively.<sup>17</sup> However, the line shapes of both bands were independent of mechanical grinding and the heating rate in our preliminary examination.

In almost all recent studies on diamond-like carbon or carbon fiber, each band has been attributed to the same phonon as graphite. These assignments are not necessarily

applicable to the heat-treated Japanese cedar samples in their present form because the formation of graphitic carbon requires considerably high temperature or high energy. Nevertheless, Raman bands were apparently observed at positions corresponding to the D- and G-bands in each heat-treated sample. In addition, above 700°C a shoulder appeared at about 1160 cm<sup>-1</sup>. Gilkes et al.<sup>18</sup> reported that a Raman band attributed to sp<sup>3</sup>-carbon in carbonaceous materials appears at the same wavenumber.

In several studies the properties of carbonaceous materials have been discussed based on Raman band parameters obtained from mathematical analyses. Some of the studies dealt with coke or coal,<sup>19-23</sup> which is expected to resemble charcoal as compared to other carbonaceous materials. Cuesta et al.<sup>23</sup> pointed out that three additional bands other than D- and G-bands can be discerned in the 1000–1800 cm<sup>-1</sup> range through curve fitting. The first band (I) due to impurity ions appears at about 1330 cm<sup>-1</sup>. A second band (D') at wavenumbers above 1605 cm<sup>-1</sup> has often been observed in graphitized materials,<sup>17,21,24-26</sup> although it was not detected in the present study. The third band (D'') is present between the D- and G-bands.

For the heat-treated Japanese cedar, we assumed that the I and D' bands are negligible but that a band (T) exists at about 1160 cm<sup>-1</sup>. Hence the Raman spectra were analyzed on the assumption that they consist of four components, expressed as T-, D-, D'', and G-bands, in the order of their wavenumbers. Thus, the best fits and reasonable values of Raman parameters were obtained for the four bands. Representative curve-fitting results of the bark heat-treated at 350°C and 1000°C are illustrated in Fig. 3. We discuss

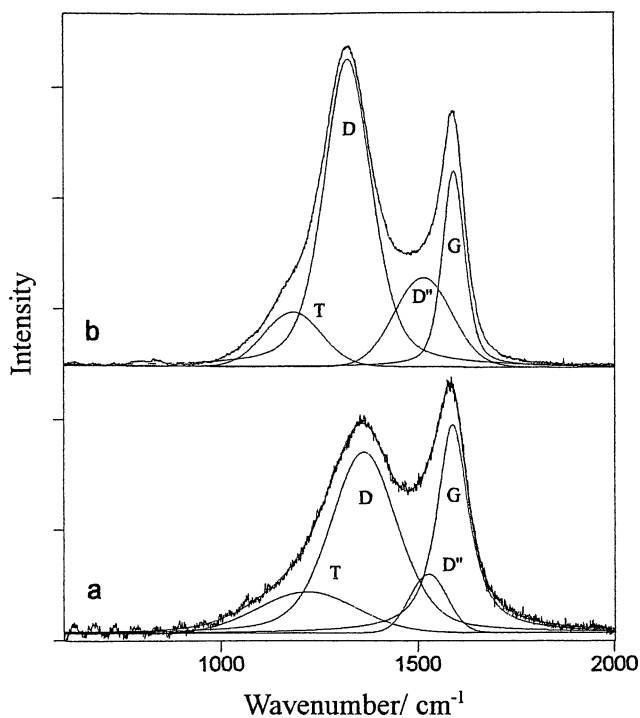


**Fig. 3a,b.** Raman spectra observed and calculated by curve-fitting of heat-treated bark. **a** 350°C. **b** 1000°C

only the Raman parameters of D- and G-bands because the parameters of the T- and D''-bands were observed to vary considerably in the samples heat-treated at the same HTT.

The plots of D- and G-band positions against HTT are illustrated in Figs. 4 and 5, respectively. The upper and lower bars correspond to the maximum and minimum values for measurements, respectively. As is evident from Figs. 4 and 5, there was no significant difference in the D- and G-band positions between the wood and bark heat-treated at each HTT. The D-band positions showed no appreciable change up to 400°C but shifted suddenly to lower wavenumbers beyond this temperature. Above 800°C, they seem again to be constant or to increase slightly. In contrast, the G-band positions shifted gradually to higher wavenumbers from 300°C to 1100°C. Green et al.<sup>20</sup> investigated the HTT dependence of Raman parameters in heat-treated coal and reported that the D-band shifted to a higher wavenumber with increasing HTT in several kinds of coal up to 1300°C, although the position of the G-band scarcely changed.

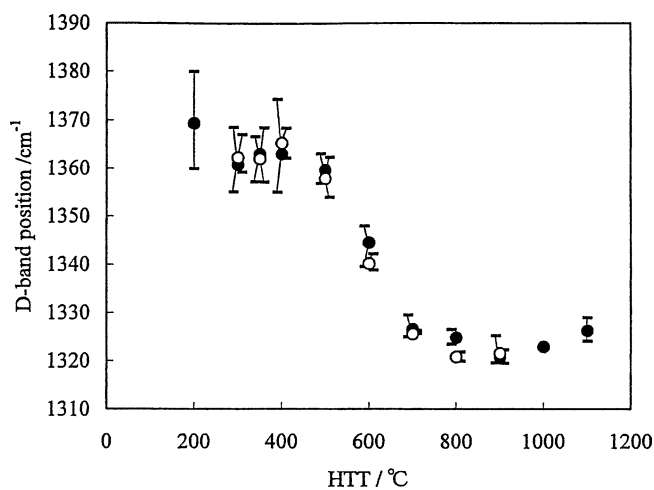


**Fig. 4.** Variation of the D-band position with heat-treatment temperature (HTT). *Open circles*, wood; *filled circles*, bark

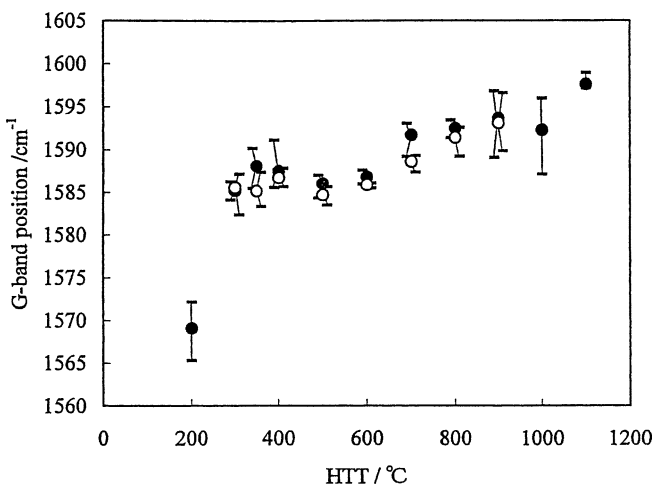


**Fig. 5.** Variation of the G-band position with HTT. *Open circles*, wood; *filled circles*, bark

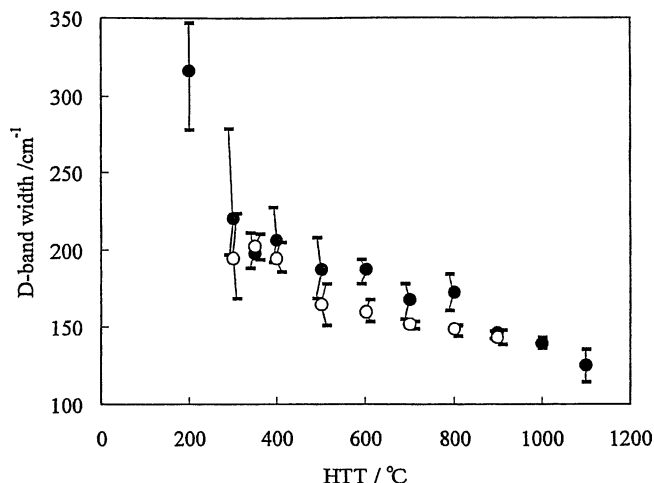


**Fig. 6.** Variation of the D-band width with HTT. *Open circles*, wood; *filled circles*, bark

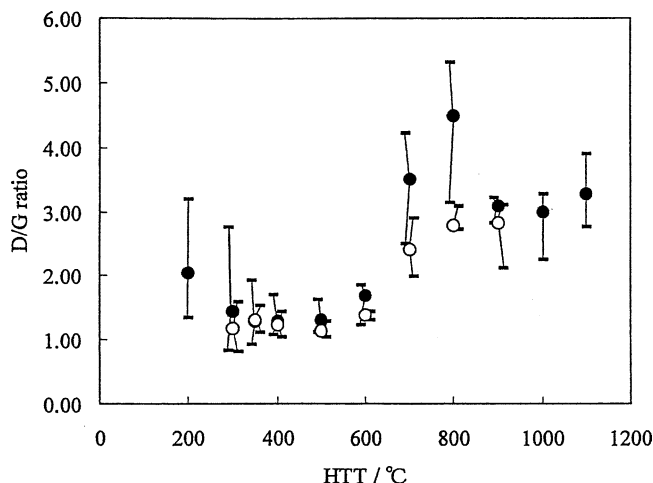


**Fig. 8.** Variation of D/G ratio with HTT. *Open circles*, wood; *filled circles*, bark

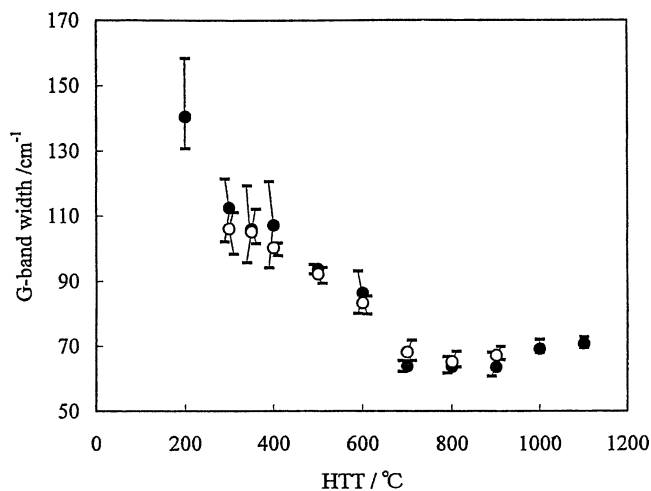


**Fig. 7.** Variation of the G-band width with HTT. *Open circles*, wood; *filled circles*, bark

Figures 6 and 7 show the plots of band width (full width at half-maximum) versus HTT. The G-band widths of wood and bark were almost compatible at each HTT. The same was mostly true for the D-band widths, although the values were slightly higher for bark than for wood at 500°–800°C.

A sudden decrease in band width was observed from 200°C to 300°C in both the D- and G-bands. Above 300°C, the D-band width decreased progressively with increasing HTT until 1100°C. The G-band width also decreased up to 800°C, and then it seemed to become constant or to increase slightly in the higher temperature range. A narrowing of band width suggests structural arrangement or ordering of elemental carbon with the rise in HTT. Thus it is apparent that the positions and the widths of both the bands had great dependence on the HTT. In particular, the D-band position and the G-band width showed marked changes in the HTT range of 400°–800°C.

The D/G ratio was calculated from each peak area, and Fig. 8 depicts its change with HTT. The D/G ratios of both

the wood and bark samples increased clearly in the HTT range of 500°–800°C. For the bark samples, it seems that the ratio reached a maximum at 800°C. The values, however, varied considerably at 700°C and 800°C, and more Raman measurements and a more reliable curve-fitting analysis are required to confirm the existence of a maximum.

Thus, we showed the correlations between HTT and the Raman parameters by irradiation of 632.1 nm light from an He-Ne laser. However, Yoshikawa et al.<sup>27</sup> reported that the D-band position and D/G ratio of graphitic carbon materials depend on the excitation wavelength; therefore, further investigations are necessary to establish whether the correlations are valid when other wavelengths are employed as an excitation light source.

As mentioned earlier, the D-band is attributable to graphitic sp<sup>2</sup>-carbon, which has reduced symmetry at the edge of the crystallite. In fact, previous studies<sup>3,24</sup> reported the absence of a D-band in a single crystal graphite and the appearance of a D-band on mechanical grinding. The crystallite diameter ( $L_a$ ) has been calculated from the D/G ratio,<sup>17,20,21,23,25,26</sup> and there is general agreement that the decrease in  $L_a$  is attributable to the increase in the intensity of the D-band relative to that of the G-band.

If this is applicable to heat-treated Japanese cedar samples, the results shown in Fig. 8 imply that  $L_a$  decreases with increasing HTT in the 400°–800°C range. Changes in the D/G ratios are consistent with those of the Freundlich parameters we reported previously,<sup>2</sup> which prove that the surface area of pyrolyzed bark increases with increasing HTT under the assumption that the edge of a crystallite is equivalent to the outer thin layers.

With respect to coals and cokes, Johnson et al.<sup>21</sup> reported that the  $L_a$  values derived from X-ray diffraction analyses increase monotonously with increasing HTT over a wide range above 300°C. They postulated that  $L_a$  obtained from the Raman spectrum does not represent the true crystallite size but, rather, the degree of coherence of the planar layers. Moreover, Wang et al.<sup>17</sup> noted, after studying pyrolytic graphite, that D-band intensity depends on the edge density

rather than the microcrystallite size. Furthermore, it can be assumed that the heat-treated Japanese cedar has extremely complex structures at the molecular level up to about 600°C because of the remaining atomic groups containing H or O. Consequently, it is difficult to apply directly the concept of crystallite diameter  $L_a$ , to the pyrolyzed Japanese cedar, although it seems that the changes in the D/G ratio with changing HTT are compatible with those of the Freundlich parameters.

## Conclusions

The Raman spectroscopic approach to the study of heat-treated Japanese cedar indicates an HTT dependence of the Raman parameters of D- and G-bands in the range of 200–1100°C. There was no significant difference in the values of any Raman parameters for the heat-treated wood and bark despite the considerable difference in the chemical components of the raw bark and wood. Accordingly, it is suggested that such correlations between the Raman parameters and HTT would be applicable to other wood species.

We have demonstrated that Raman spectroscopy has the potential to be a useful, convenient microscopic technique for evaluating HTT during the preparation of charcoal. HTT can be roughly estimated from the overall Raman parameters of the D- and G-bands. This estimation is expected to be helpful in preventing the contamination of dioxins when charcoal is produced from lignocellulosics, especially waste wood-based materials including synthetic resins, because the thermal decomposition of dioxins is not accelerated until the temperature is raised above 700–800°C. To extend the applicability of the HTT estimation based on Raman measurement, we are currently studying other wood and lignocellulosic species.

## References

- Kurimoto Y, Novicio LP, Doi S, Aoyama M (2000) Improved adsorption potential of Sugi (*Cryptomeria japonica* D. Don) bark carbonized after steam-treatment. *Mater Sci Res Int* 6:63–64
- Kurimoto Y, Doi S, Aoyama M (2001) Removal of trichloroethylene from aqueous solution by pyrolyzed Japanese cedar bark. *J Wood Sci* 47:76–79
- Tuinstra F, Koenig JI (1970) Raman spectra of graphite. *J Chem Phys* 53:1126–1130
- Yamauchi S, Kikuchi Y, Kurimoto Y (2000) Raman spectral changes of sugi bark during thermal degradation and carbonization. *Mater Sci Res Int* 6:227–228
- Darmstadt H, Pantea D, Sümmchen L, Roland U, Roy C (2000) Surface and bulk chemistry of charcoal obtained by vacuum pyrolysis of bark: influence of feedstock moisture content. *J Anal Appl Pyrolysis* 53:1–17
- Yamauchi S, Koizumi A, Kurimoto Y, Tamura Y (1997) Vibrational spectroscopic study on wood and wood-based materials. II. Infrared and Raman spectroscopic investigation for MDI penetration behavior in wood (in Japanese). *J Adhes Soc Jpn* 33:95–102
- Yamauchi S, Tamura Y, Kurimoto Y, Koizumi A (1997) Vibrational spectroscopic study on wood and wood-based materials. III. Identification of adhesives in wood by using FT-Raman spectroscopy as a nondestructive analytical method (in Japanese). *J Adhes Soc Jpn* 33:380–387
- Yamauchi S, Tamura Y, Kurimoto Y, Koizumi A (1999) Vibrational spectroscopic study on wood and wood-based materials. IV. Solvent effects of diluent on MDI penetration behavior in wood (in Japanese). *J Adhes Soc Jpn* 35:300–308
- Laks PE (1990) Chemistry of bark. In: Hon DNS, Shiraiishi N (eds) *Wood and cellulosic chemistry*. Marcel Dekker, New York, pp 262–269
- Laver ML (1991) Bark. In: Lewin M, Goldstein IS (eds) *Wood structure and composition*. Marcel Dekker, New York, pp 418–421
- Sjöström E (1992) *Wood chemistry: fundamentals and applications*. Academic, San Diego, p 113
- Graham RG, Bergougnou MA, Overend RP (1984) Fast pyrolysis of biomass. *J Anal Appl Pyrolysis* 6:95–135
- Migita N (1968) Composition of wood. In: Migita N, Yonezawa Y, Kondo T (eds) *Wood chemistry I* (in Japanese). Kyoritsu Syuppan, Tokyo, p 72
- Uemura T (ed) (1973) *Handbook of wood technology* (in Japanese). Maruzen, Tokyo, pp 215–217
- Oren MJ, Nassar MM, MacKay GDM (1983) Infrared study of inert carbonization of spruce wood lignin under helium atmosphere. *Can J Spectrosc* 29:10–12
- Kato Y, Umehara K, Aoyama M (1997) An oil sorbent from wood fiber by mild Pyrolysis. *Holz Roh Werkst* 55:399–401
- Wang Y, Alsmeyer DC, McCreery RL (1990) Raman spectroscopy of carbon materials: structural basis of observed spectra. *Chem Mater* 2:557–563
- Gilkes KWR, Sands HS, Batchelder DN, Milne WI, Robertson J (1998) Direct observation of  $sp^3$  bonding in tetrahedral amorphous carbon UV Raman spectroscopy. *J Noncryst Solids* 227–230:612–616
- Nakamizo M, Honda H, Inagaki M, Hishiyama Y (1977) Raman spectra, effective Debye parameter and magnetoresistance of graphitized cokes. *Carbon* 15:295–298
- Green PD, Johnson CA, Thomas KM (1983) Application of laser Raman microprobe spectroscopy to the characterization of coals and cokes. *Fuel* 62:1013–1023
- Johnson CA, Patrick JW, Thomas KM (1986) Characterization of coal chars by Raman spectroscopy, X-ray diffraction and reflectance measurements. *Fuel* 65:1284–1290
- Angoni K (1992) Remarks on the structure of carbon materials on the basis of Raman spectra. *Carbon* 31:537–547
- Cuesta A, Dhamelincoourt P, Laureyns J, Martinez-Alonso A, Tascon JMD (1994) Raman microprobe studies on carbon materials. *Carbon* 32:1523–1532
- Nakamizo M, Honda H, Inagaki M (1978) Raman spectra of ground natural graphite. *Carbon* 16:281–283
- Lespade P, Al-Jishi R, Dresselhaus MS (1982) Model for Raman scattering from incompletely graphitized carbons. *Carbon* 20:427–431
- Dillon RO, Woollam JA, Katkanant V (1984) Raman scattering to investigate disorder and crystallite formation in as-deposited and annealed carbon films. *Phys Rev B* 29:3482–3489
- Yoshikawa M, Katagiri G, Ishida H, Ishitani A (1988) Raman spectra of diamondlike amorphous carbon films. *Solid State Commun* 66:1177–1180